FTIR reveals structural differences between native β-sheet proteins and amyloid fibrils

GIORGIA ZANDOMENEGHI,[1] MARK R.H. KREBS,[2] MARGARET G. MCCAMMON,[3] AND MARCUS FÄNDRICH[1]

[1]Institut für Molekulare Biotechnologie (IMB), D-07745 Jena, Germany
[2]Polymers and Colloids (P&C) Group, Cavendish Laboratory, and [3]Department of Chemistry, University of Cambridge, Cambridge, United Kingdom

(RECEIVED July 30, 2004; FINAL REVISION August 26, 2004; ACCEPTED August 26, 2004)

Abstract

The presence of β-sheets in the core of amyloid fibrils raised questions as to whether or not β-sheet-containing proteins, such as transthyretin, are predisposed to form such fibrils. However, we show here that the molecular structure of amyloid fibrils differs more generally from the β-sheets in native proteins. This difference is evident from the amide I region of the infrared spectrum and relates to the distribution of the ϕ/ψ dihedral angles within the Ramachandran plot, the average number of strands per sheet, and possibly, the β-sheet twist. These data imply that amyloid fibril formation from native β-sheet proteins can involve a substantial structural reorganization.

Keywords: protein structure/folding; prions; aggregation; amyloid; conformational disease; infrared spectroscopy

Amyloid fibrils are polypeptide aggregates that can be formed in the course of degenerative conditions, such as Alzheimer's and Creutzfeldt-Jakob diseases. X-ray fiber diffraction shows that amyloid fibrils encompass a specific type of β-sheet arrangement, termed cross-β (Serpell et al. 1999). This structure has been suggested to represent a generic conformational state that can be adopted by many, if not all polypeptide main chains (Chiti et al. 1999; Fandrich and Dobson 2002), and which is distinct from a globular protein, the product of native protein folding encoded within the genetic sequence. However, polypeptides can vary tremendously in the conditions most optimal for amyloid formation, with some being extremely nonphysiologic. Amyloid fibrils can be formed from polypeptides that fold into native proteins lacking β-sheets, such as myoglobin (Fandrich et al. 2003), or that are intrinsically unable to fold as monomers, such as polyamino acids (Fandrich and Dobson 2002; Perutz et al. 2002). In addition, they can be formed from polypeptides that fold into native states with extensive β-sheet structure, such as the 127-residue protein transthyretin (TTR).

These observations raised questions as to whether native β-sheet proteins might be predisposed to form amyloid fibrils and whether their structure is retained during fibril formation. Structural models have been proposed suggesting that TTR fibrils consist of globular protein units with a conformation that is almost identical to the fully native one (Sebastiao et al. 1998; Eneqvist et al. 2000). The solvent exposure of many residues is similar in both states (Serag et al. 2001). Moreover, familial amyloidosis can be associated with mutations, such as Val30Met, that have small effects on the fold of the globular protein, although some decrease the thermodynamic stability of this conformation (Kelly et al. 1997).

Fourier-transform infrared (FTIR) spectroscopy has revealed, however, that native β-sheet proteins are associated with amide I bands that can differ significantly from those obtained in the analysis of inclusion bodies or thermally induced aggregates (Oberg et al. 1994; Fink 1998). Amide I (measured in H_2O) or amide I′ components (in D_2O) occur in the wavenumber range of from 1600 cm^{-1} to 1700 cm^{-1} and arise primarily from stretching vibrations of main-chain

Reprint requests to Marcus Fändrich, Institut für Molekulare Biotechnologie (IMB), Beutenbergstraße 11, D-07745 Jena, Germany; e-mail: fandrich@imb-jena.de; fax: +49-3641-656310.

Abbreviations: TTR, transthyretin; FTIR, fourier-transformed infrared; NMR, Nuclear Magnetic Resonance; EM, Electron Microscopy.

Article published online ahead of print. Article and publication date are at http://www.proteinscience.org/cgi/doi/10.1110/ps.041024904.

carbonyl groups. Their sensitivity to secondary structural context and dihedral torsional angles ϕ/ψ provides direct structural information about the polypeptide backbone (Susi et al. 1967; Timasheff et al. 1967; Krimm and Bandekar 1986; Jackson and Mantsch 1991). Although FTIR lacks the high resolving power of X-ray crystallography or nuclear magnetic resonance (NMR), it presents the advantages of fast-time response and wider applicability required for studying aggregated materials with natural isotope distribution. Here, we have used FTIR to explore the molecular conformations of the native form and amyloid fibrils formed from TTR and other polypeptide chains.

Results

Native β-sheet proteins and amyloid fibrils differ in the amide I band

Transmission mode FTIR spectra were recorded using D_2O solutions of recombinant TTR. Native TTR (Fig. 1B) has an absorption spectrum with a broad amide I′ band with a maximum at 1630 cm^{-1} (Fig. 1A). TTR fibrils, in contrast, produce a spectrum with a narrower amide I′ band with a maximum at 1615 cm^{-1} (Fig. 1C,D) and an additional low-intensity peak at 1684 cm^{-1}. Although the FTIR spectra indicate that both structural forms of TTR contain large amounts of the extended conformation (Krimm and Bandekar 1986; Susi and Byler 1987), the different position of the amide I maxima suggests that the two states do not have the same structure (see below). A literature survey of amide I′ data recorded on amyloid fibrils and globular proteins with at least 30% β-sheet structure (Table 1) revealed that these effects are not specific to TTR. In fact, amyloid fibrils and native β-sheet proteins have maxima within two characteristic, although partially overlapping, spectral regions (Fig. 2). The range of amyloid fibrils extends from 1611 cm^{-1} to 1630 cm^{-1}, whereas native β-sheet proteins produce amide I′ peaks clustering between 1630 cm^{-1} and 1643 cm^{-1}. In addition, there are also differences in shape of the amide I′ band, in that native β-sheet proteins have broader maxima. In two cases, namely TTR and ubiquitin, FTIR spectra have been recorded using the same polypeptide chain in the two conformations.

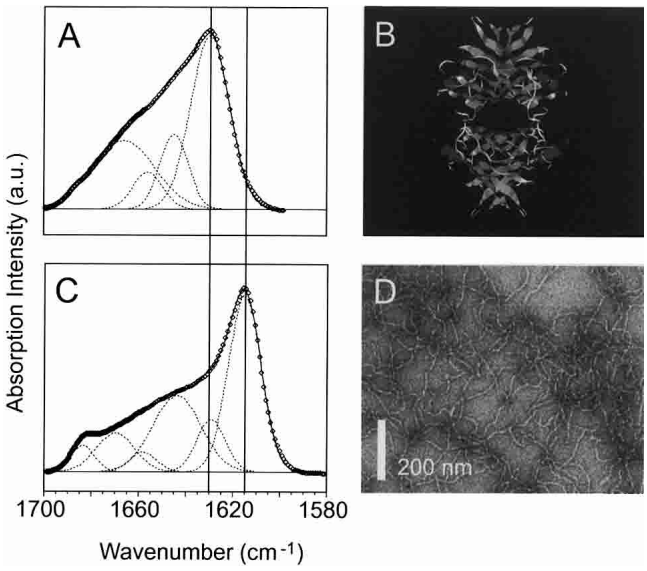

Figure 1. Structure of native TTR and TTR amyloid fibrils. Amide I′ region from the FTIR spectrum of native TTR (*A*). Ribbon diagram of the native TTR tetramer (PDB code 1RLB). Helices are colored dark gray, β-sheets are colored light gray, and loops are white (*B*). Amide I′ region (*C*) and EM image (*D*) of TTR amyloid fibrils. Experimental infrared data points are displayed as diamonds. The individual components of the curve fit are displayed with dotted lines. Their sum (continuous line) overlaps the experimental data closely.

The spectral characteristics described above do not depend on the presence of deuterons, for similar transitions were also observed for the normal thermal aggregation of native β-sheet proteins, such as interleukin-1β, when using attenuated total reflectance FTIR spectroscopy and fully protonated samples (Oberg et al. 1994). Furthermore, simple oligomerization cannot account for these effects too, as was shown recently for the native β-sheet protein lithostathine that assembles into nonamyloid fibrils by oligomerization of globular protein units and without significant changes in its amide I band (Laurine et al. 2003).

Component analysis of the spectra recorded on the two structural states of TTR (Fig. 1A,C) shows that the β-sheet content of the fibril is insignificantly larger (54%) compared with the native state (53%), thus indicating that the higher amide I′ maximum of native TTR is not due to the overlap with a more intense band at higher wavenumbers arising from non-β structures. Some amyloid fibrils can have a β-sheet content of only 35% and an amide I′ maximum at 1617 cm^{-1} (Fandrich et al. 2003), whereas some proteins have a β-sheet content >50% and an amide I′ maximum at 1643 cm^{-1} (Table 1). We conclude that the spectral and structural differences of two forms of TTR are inherent to properties of their β-sheet structure.

Amyloid fibrils populate a specific region of the Ramachandran plot

Early investigations suggested that FTIR spectroscopy might be able to distinguish parallel from antiparallel β-sheets, in that the latter possess amide I′ maxima at smaller wavenumbers along with a low-intensity peak around 1685 cm^{-1} (Toniolo and Palumbo 1977; Krimm and Bandekar 1986). Although these antiparallel properties are observed in many amyloid fibril samples, implying that these might be constituted of antiparallel β-sheets, the low-frequency component present in amyloid fibril samples has been related to residual amounts of nonfibrillar material

Table 1. *Structural parameters and infrared data of globular β-sheet proteins and amyloid structures*

Sequence	PDB code	β-sheet content (%)	Average no. of strands/sheet	Parallel β-sheet content (%)	Twist angle δ (°)	Amide I′ maximum (cm^{-1})	Reference
Native proteins							
Avidin	1RAV	50	8.0	0	37	1633	(Swamy et al. 1996)
Azurin	1JOI	34	4.0	36	33	1638	(Surewicz et al. 1987)
Basic Fibroblast Growth Factor	2FGF	39	5.2	0	51	1643	(Dukor et al. 1992)
Choleratoxin Subunit B	1JR0	37	6.0	0	38	1633	(Surewicz et al. 1990)
Green Fluorescence Protein	1EMA	51	11.0	12	27	1630	(Fukuda et al. 2000)
Intestinal Fatty-acid Binding Protein	2IFB	59	10.0	0	31	1631	(Muga et al. 1993)
β-Lactoglobulin A	1QG5	44	10.0	0	32	1634	(Dong et al. 1996)
Platelet Derived Growth Factor	1PDG	51	2.5	0	43	1643	(Prestrelski et al. 1991)
Porcine Pancreatic Elastase	1QNJ	34	7.0	0	50	1636	(Byler et al. 1995)
Ribonuclease	1KF5	33	3.5	0	41	1637	(Panick and Winter 2000; R. Winter, pers. comm.)
Serum Amyloid P Component	1SAC	44	8.0	0	28	1633	(Dong et al. 1994)
Staphylococcal Nuclease	1STN	30	5.6	0	49	1631	(From and Bowler 1998)
Tendamistat	1HOE	46	3.0	0	49	1635	(Zscherp et al. 2003)
Transthyretin	1F41	53	9.0	15	35	1630	This study
Ubiquitin	1UBQ	32	5.0	26	48	1642	M. Fandrich, unpubl.
Amyloid structures							
Aβ(1–40)						1625	(Fraser et al. 1992)
Acylphosphatase						1613	(Chiti et al. 1999)
ADA2h						1615	(Villegas et al. 2000)
Amylin 17–37						1626	(Nilsson and Raleigh 1999)
Calcitonin						1620	(Arvinte et al. 1993)
Csp-1						1620	(Wilkins et al. 2000)
Glucagon						1613	M. Fandrich, unpubl.
Lysozyme Asp67His						1630	(Booth et al. 1997)
Insulin						1628	(Bouchard et al. 2000)
Myoglobin						1617	(Fandrich, et al. 2003)
Peptide: $(DPKG)_2$-$(VT)_7$-GKGDPKPD						1621	(Janek et al. 1999)
Peptide: QG-A_7-GQ						1622	M. Fandrich, unpubl.
Peptide: STVIIE						1625	(Lopez De La Paz et al. 2002)
PolyT						1614	(Fandrich and Dobson 2002)
PolyK						1611	(Fandrich and Dobson 2002)
PolyE						1616	(Fandrich and Dobson 2002)
SHa PrP 109–12						1623	(Nguyen et al. 1995)
SH3						1618	(Zurdo et al. 2001)
Transthyretin						1615	This study
Ubiquitin						1615	M. Fandrich, unpubl.

rather than to the amyloid core structure itself (Zurdo et al. 2001). In addition, solid-state NMR spectroscopy and X-ray diffraction show that several amyloid fibrils possess parallel β-sheets (Blake and Serpell 1996; Antzutkin 2004), and increasing experimental and theoretical studies argue that the properties mentioned above do not represent a general discrimination between parallel and antiparallel β-sheets (Susi and Byler 1987; Kubelka and Keiderling 2001; Barth and Zscherp 2002).

Therefore, we investigated whether the FTIR spectral differences between β-sheets in globular proteins and amyloid fibrils in Figure 2 arise from other conformational properties of the β-sheets, for example, a different distribution of the ϕ/ψ dihedral angles. Solid-state NMR studies provided the ϕ/ψ angles for the amyloid fibrils from the two peptides, that is, TTR(105–115), which corresponds to residues 105–115 of transthyretin (Jaroniec et al. 2002, 2004) and Aβ(1–40) (Petkova et al. 2002). Comparing the Ramachandran plots of native TTR (or other native β-sheet proteins) and the two amyloid structures, differences in the population of the β-sheet region become evident (Fig. 3A,B). Whereas the ϕ/ψ pairs for native TTR sample most of the area that represents β-sheet structure and that extends mainly to the right side of the diagonal (Fig. 3A), ϕ/ψ pairs for TTR(105–115) and Aβ(1–40) are characterized by a narrow distribution close to the diagonal $\psi = -\phi$ (Fig. 3B).

Figure 3C shows a comparison of the torsional angles of residues 105–115 in TTR(105–115) amyloid fibrils and in

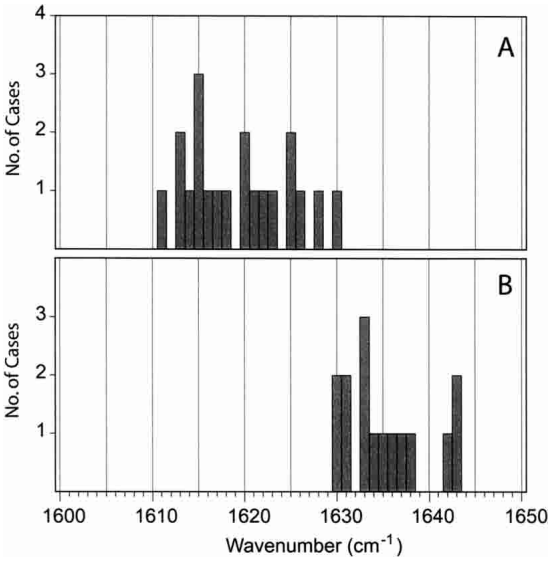

Figure 2. Amide I′ maxima of native β-sheet proteins and amyloid fibrils. Spectral position of the amide I′ maxima of amyloid fibrils (*A*) and native β-sheet proteins (*B*), taken from Table 1.

the context of globular full-length TTR. The most significant changes occur in residues Ile 107, Ser 112, Pro 113, and Tyr 114 (Fig. 3C). Pro 113 and Tyr 114 are not part of the β-sheet structure in the native state, but revert to an extended conformation upon fibril formation. Even comparing the ϕ/ψ pairs of residues 106–112, which adopt the extended conformation in both states, TTR(105–115) amyloid fibrils show a smaller spread of the ϕ/ψ pairs compared with native TTR (Fig. 3D) and occur in closer proximity to the $\psi = -\phi$ diagonal. Figure 3, C and D, shows that the same residues can be present as β-sheet structure in the amyloid fibrils and in the native conformation, and differ in structure nevertheless. Taken together, we conclude that the residues constructing the amyloid fibril core have a greater structural homogeneity. The restricted distribution of the ϕ/ψ pairs within the β-sheet region of the Ramachandran plot is also consistent with the narrower amide I′ bands of amyloid fibrils (see above), and supports the view that the spectroscopic differences between native β-sheet proteins and amyloid fibrils relate to properties inherent in their β-sheets.

The amide I′ maximum relates to the β-sheet twist and the number of strands per sheet

All native β-sheet proteins are characterized by a right-hand twist of the β-sheets when viewed along the chain axis (Chothia 1973; Chou et al. 1982; Salemme 1983). The sheet twist manifests itself in terms of a strand twist, that is, a rotation of the backbone hydrogen-bond donor and acceptor groups around the strand axis. This property is associated with ϕ/ψ pairs extending largely toward the right side of the $\psi = -\phi$ diagonal in the Ramachandran plot, whereas planar β-sheets have ϕ/ψ pairs close to the diagonal (Chothia 1973). To test whether the amide I′ characteristics might be affected by the twist angle, we have analyzed the set of native β-sheet proteins described in Table 1, where the amide I′ maximum can be readily related to the molecular structure. The average twist angles δ of these proteins range from 28° to 51°, which is in good agreement with literature data (Richardson 1981; Yang and Honig 1995). When comparing δ with the amide I′ maxima, larger twist angles are correlated with maxima at higher wavenumbers (Fig. 4A). A linear fit gives an R-value of 0.68, which improves even to 0.79 if the data set is restricted to crystal structures of ≤2 Å resolution. In addition, we found that the amide I′ maximum of native β-sheet proteins depends also on the average number of strands per β-sheet (Fig. 4B), in that small sheets produce amide I′ maxima at higher wavenumbers. The twist angle and the number of strands per sheet are related properties, as it is known that β-sheets consisting of only few β-strands are associated with larger twist angles than β-sheets containing a large number of strands (Richardson

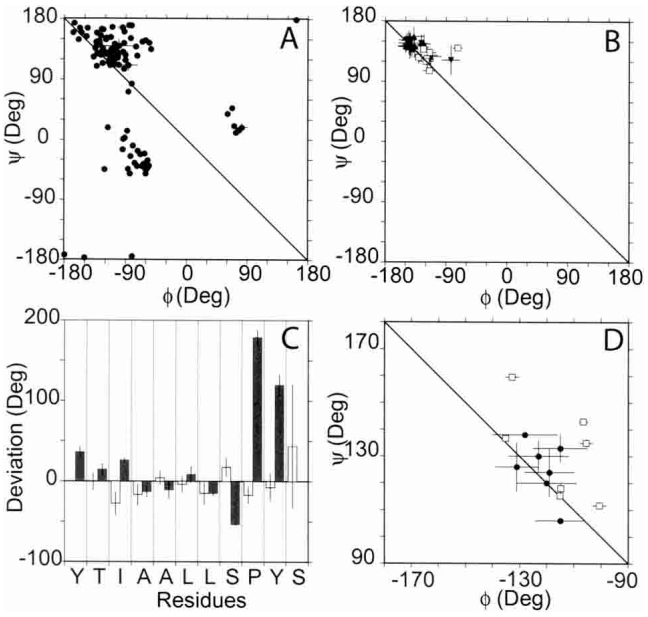

Figure 3. Comparison of the (ϕ,ψ) dihedral angles in native β-sheet proteins and amyloid fibrils. (*A*,*B*) Ramachandran plots of native TTR (*A*) and amyloid fibrils formed from TTR(105–115) (□) and Aβ(1–40) (▲ and ▼) (*B*). For Aβ(1–40) two sets of (ϕ,ψ) measurements were reported (Petkova et al. 2002). Errors in *A* and *D* represent the deviation of ϕ,ψ when comparing the two protein molecules in the asymmetric unit. Often the errors are smaller than the symbol size. Residues 98–103 were omitted in the plot (*A*) because they form loops of evidently different structure. (*C*) Deviation of ϕ (open bars) and ψ (filled bars) angles of TTR(105–115) amyloid fibrils compared with the respective residues in native TTR. The ϕ angle of Pro 113 in the amyloid structure was calculated from the structural ensemble in the PDB-file 1RVS. (*D*) Ramachandran plots of residues 106–112 in native TTR (□) and TTR(105–115) amyloid fibrils (●).

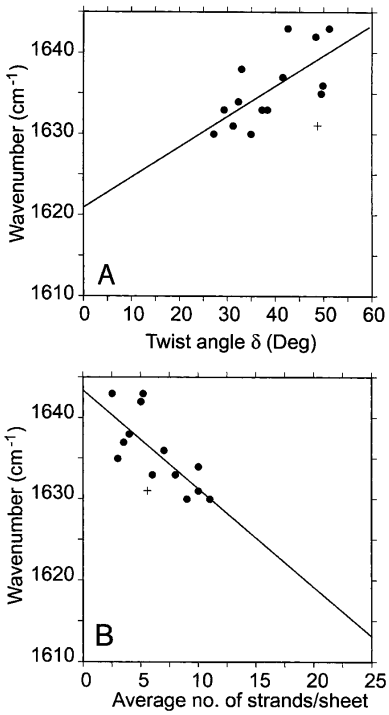

Figure 4. Comparison of the amide I′ maximum with the twist angle and the number of strands. Correlation between the amide I′ maximum and the twist angle δ for native β-sheet proteins in Table 1 (*A*). Data points fit with $\nu = 1621 + 0.4 \cdot \delta$, where ν is the amide I′ maximum (R-value 0.68). Correlation between the amide I′ maxima of native β-sheet proteins and the average number of strands per sheet, s (*B*). Data can be fitted with the curve $\nu = 1643 - 1.2 \cdot s$, R-value: 0.75. Staphyloccal nuclease (+) was not included in the fit, as the extraordinary difference (18 cm^{-1}) of the amide I maximum between the H_2O and D_2O spectrum (From and Bowler 1998), indicates that D_2O samples are affected by factors that this analysis does not take into account, such as structural rearrangements during deuteration.

1981). Consistent with this, ab initio calculations have shown that the amide I′ maximum will be shifted to higher wavenumbers if the number of strands per β-sheet decreases, or if the twist angle is increased (Kubelka and Keiderling 2001). At present, it cannot be decided, however, whether the correlations shown in Figure 4 depend on the parallel or antiparallel nature of the underlying β-sheets, because the native protein structures available for this analysis (Table 1) are dominated by antiparallel β-sheets.

Extrapolating the correlations from Figure 4 also to wavenumbers below 1630 cm^{-1} predicts that amyloid fibrils would possess β-sheets that differ from native β-sheet proteins by having smaller twist angles and a larger number of strands. Whereas the latter property is clearly associated with amyloid fibrils, it is much more difficult to assess, in the absence of information on the quaternary structure of amyloid fibrils at atomic resolution, the possible involvement of δ. The presently available NMR data on the structure of amyloid fibrils lead to twist angles of $\delta = 26° \pm 24°$ for TTR(105–115) fibrils, and $\delta = 14° \pm 37°$, as well as $\delta = 17° \pm 38°$ for the two data sets of Aβ(1–40) (Petkova et al. 2002). In spite of large errors, all values would appear within a range of δ angles as would be predicted by the correlation in Figure 4A. In addition, we have considered the spectrum of amyloid fibrils formed by an Ala-rich peptide (sequence QG-A_7-GQ, Table 1) with an amide I′ maximum of 1622 cm^{-1}. It is known that β-poly-L-Ala is a pleated structure with $\delta \approx 0°$ (Arnott et al. 1967), again indicating that the correlation in Figure 4A holds also for amyloid fibrils. Taken together, we propose that amyloid fibrils and native β-sheet proteins produce different amide I′ bands, as they differ by the structural variability of the residues constructing their sheets, the average number of strands per sheet, and the twist angles. It is of note that the latter conclusion is supported independently by cryo-electron microscopy, which also has suggested that amyloid fibrils have smaller twist angles compared with native proteins (Jimenez et al. 2002).

Discussion

We show here that amyloid fibrils and native β-sheet proteins can be distinguished on the basis of the amide I′ region of their infrared spectra. Although both structural forms are evidently composed of β-sheet structure, FTIR data indicate that these β-sheets are generally different. Interestingly, inclusion bodies and thermally induced nonfibrillar aggregates have the same type of infrared spectrum as the one presented here for amyloid fibrils (Jackson and Mantsch 1991; Fink 1998), suggesting that these various aggregated states represent a common group of structures, alternative to native β-sheet proteins.

The amide I′ maxima of native β-sheet proteins correlate with the average number of strands and the β-sheet twist. Of course, the present analysis cannot compare individual secondary structural elements, such as specific strands, and we have examined globally averaged structural properties. This reveals that β-sheet structure absorbs in a very broad spectral range, and indeed, the residues present in the β-sheets of natural proteins can vary substantially in their ϕ/ψ dihedral angles. This heterogeneity is reduced in the amyloid fibril, and these sheets possess more strands and, possibly, a smaller twist angle. However, the variability of the observed maxima implies that this correlation is modulated by additional factors.

We believe that these findings have three major implications. First, they might enable applications of infrared spectroscopy in the clinical diagnosis of amyloid, for example, by using FTIR-microscopes (Choo et al. 1996). Second, the general spectroscopic difference between amyloid fibrils and native β-sheets suggests that they represent different types of structure, and that a substantial structural reorganization is necessary to form amyloid fibrils from a native β-sheet protein. The experimentally verified amyloid fibril

structures from transthyretin and the SH3-domain from PI3-kinase cannot be explained with the native structure of these proteins (Blake and Serpell 1996; Jimenez et al. 1999). Moreover, increasing evidence suggests that amyloid fibril formation involves the disruption of a significant fraction of the native contacts in conjunction with an at least partial unfolding of the native structure (Fandrich et al. 2003). Finally, our study promotes ideas that it is possible to develop therapeutic agents that act specifically on amyloid structures by inhibiting their formation, but which do not impair the folding of native β-sheet proteins.

Materials and methods

Preparation and analysis of transthyretin samples

Transthyretin was obtained by using a recombinant expression scheme (McCammon et al. 2002). Labile hydrogens of TTR were replaced with deuterium by repeated cycles of dissolving in D_2O solution and lyophilization. The spectrum of native TTR was recorded using a freshly dissolved solution of the protein (10 mg/mL) in D_2O (pD 6.75). pD adjustments were carried out using DCl or NaOD solutions (Sigma). All pD values were not isotope corrected. Amyloid fibrils were formed by incubation of 10 mg/mL TTR in D_2O (pD 2.0) for 3 d at 37°C. Nonaggregated material was removed by centrifugation before recording the FTIR spectrum. Presence of amyloid fibrils was demonstrated with negative stain electron microscopy as described previously (Fandrich and Dobson 2002).

Spectra were collected at room temperature using a FTS 175C FT-IR spectrometer (Bio-Rad) equipped with a cryogenic MCT detector cooled in liquid nitrogen. Sample aliquots were placed between CaF_2 windows separated by a 50-μm polyethylene terephthalate spacer (Goodfellow). The sample compartment was thoroughly purged with dry nitrogen. Spectra represent averages of 256 scans recorded between 3000 cm^{-1} and 1000 cm^{-1}. Fitting of the amide I′ band was performed using Lorentzian and Gaussian curves.

Construction of libraries of native β-sheet proteins and amyloid fibrils

To create the libraries of native β-sheet proteins and amyloid fibrils reported in Table 1, we used amide I′ absorption maxima, including only original spectra from literature data. In addition, all spectra were recorded in the transmission mode. The native β-sheet proteins in our libraries possess a native β-sheet content of at least 30%, on the basis of the Promotif definitions implemented in the PDBsum directory (http://www.biochem.ucl.ac.uk/bsm/pdbsum). This definition considers only residues present in β-sheets, but it excludes ϕ/ψ pairs that occur within the β-region of the Ramachandran plot, and are located in turns of the tertiary structure. We have tried, alternatively, to relate the FTIR properties with δ values obtained by averaging all ϕ/ψ pairs within the β-sheet region, hence, including residues that are not actually located in β-sheets, but which have similar ϕ/ψ pairs. However, this definition decreased the correlation substantially. Finally, in the libraries, cases of sequential or structural homology were excluded by using no more than one example per protein family, on the basis of the definitions of the SCOP database (http://scop.mrc-lmb.cam.ac.uk/scop/). In the case of the amyloid fibrils, we excluded homologous sequences or data from smaller sequence fragments if the spectrum of a larger sequence region was also available.

Structural analysis of native β-sheet proteins

All native β-sheet protein structures used in this analysis were obtained by X-ray crystallography. The β-sheet content and the average number of strands per β-sheet are based on the definitions from Promotif (PDBsum database, http://www.biochem.ucl.ac.uk/bsm/pdbsum). In the case of proteins containing more than one β-sheet, these averages were weighted for the number of residues in each sheet. Cholera toxin subunit B, a complex containing intermolecular β-sheets, had to be defined manually to encompass six strands per sheet. The parallel strands content in Table 1 has been determined as the number of backbone-to-backbone hydrogen bonds between parallel strands, relative to the total number of hydrogen bonds connecting strands in the β-sheet, using the hydrogen bonds definition of RasMol (Sayle and Milner-White 1995). The average twist angle δ was computed in all cases from the dihedral angles (ϕ, ψ) of those residues that are present in β-sheets and occur within the second quadrant of the Ramachandran plot ($-180° \le \phi \le 0°$ and $180° \le \psi \le 0°$). If the asymmetric unit contains more than one protein subunit, the δ value was averaged over all subunits and weighted for the β-sheet content if different in the various subunits. The twist angle δ was calculated as a function of the dihedral angles (ϕ, ψ, ω) (Chou et al. 1982; Shamovsky et al. 2000). With the assumption, $\omega = -180°$, that is, all peptide bonds are present in a *trans* conformation, δ was approximated from the expression

$$\sin(\delta/4) = -0.814 \cdot \sin\left(\frac{\phi+\psi}{2}\right) + 0.030 \cdot \sin\left(\frac{\phi-\psi}{2}\right)$$

(Chou and Scheraga 1982; Chou et al. 1982). It is difficult to estimate the error of these measurements and to compare them between NMR data sets (amyloid fibrils) and crystal structures (native proteins). In the latter case, we obtained an estimate of the δ errors by comparison with crystal structures containing more than two protein subunits in the asymmetric unit and their deviation of the ϕ/ψ angles, depending on the resolution. On the basis of this analysis, we obtained errors (Δδ) of 1.6° (resolution ≤2 Å) or 3.5° (resolution >2 Å). In contrast, the errors Δδ were calculated for the amyloid fibril data from the errors on ϕ/ψ of each residue, as measured by NMR (Petkova et al. 2002; Jaroniec et al. 2004). It is worthwhile to notice, however, that the distribution of the δ values is very narrow, compared with the substantial errors obtained with this method, thus raising the question whether using the errors on ϕ/ψ from the NMR data overestimates the true errors Δδ.

Acknowledgments

M.F. and G.Z. acknowledge a BioFuture grant from the Bundesministerium für Bildung und Forschung (BMBF). M.R.H.K. acknowledges funding from the EPSRC. We thank A. Lehmann for her assistance in evaluating the protein data, and C.M. Dobson, H. Mantsch, C.V. Robinson, K. Wieligmann, and M. Zacharias for helpful discussions and support.

References

Antzutkin, O.N. 2004. Amyloidosis of Alzheimer's Aβ peptides: Solid-state nuclear magnetic resonance, electron paramagnetic resonance, transmission

electron microscopy, scanning transmission electron microscopy and atomic force microscopy studies. *Magn. Reson. Chem.* **42:** 231–246.

Arnott, S., Dover, S.D., and Elliott, A. 1967. Structure of β-poly-L-alanine: Refined atomic co-ordinates for an anti-parallel β-pleated sheet. *J. Mol. Biol.* **30:** 201–208.

Arvinte, T., Cudd, A., and Drake, A.F. 1993. The structure and mechanism of formation of human calcitonin fibrils. *J. Biol. Chem.* **268:** 6415–6422.

Barth, A. and Zscherp, C. 2002. What vibrations tell us about proteins. *Q. Rev. Biophys.* **35:** 369–430.

Blake, C. and Serpell, L. 1996. Synchrotron X-ray studies suggest that the core of the transthyretin amyloid fibril is a continuous β-sheet helix. *Structure* **4:** 989–998.

Booth, D.R., Sunde, M., Bellotti, V., Robinson, C.V., Hutchinson, W.L., Fraser, P.E., Hawkins, P.N., Dobson, C.M., Radford, S.E., Blake, C.C., et al. 1997. Instability, unfolding and aggregation of human lysozyme variants underlying amyloid fibrillogenesis. *Nature* **385:** 787–793.

Bouchard, M., Zurdo, J., Nettleton, E.J., Dobson, C.M., and Robinson, C.V. 2000. Formation of insulin amyloid fibrils followed by FTIR simultaneously with CD and electron microscopy. *Protein Sci.* **9:** 1960–1967.

Byler, D.M., Wilson, R.M., Randall, C.S., and Sokoloski, T.D. 1995. Second derivative infrared spectroscopy as a non-destructive tool to assess the purity and structural integrity of proteins. *Pharm. Res.* **12:** 446–450.

Chiti, F., Webster, P., Taddei, N., Clark, A., Stefani, M., Ramponi, G., and Dobson, C.M. 1999. Designing conditions for in vitro formation of amyloid protofilaments and fibrils. *Proc. Natl. Acad. Sci.* **96:** 3590–3594.

Choo, L.P., Wetzel, D.L., Halliday, W.C., Jackson, M., LeVine, S.M., and Mantsch, H.H. 1996. In situ characterization of β-amyloid in Alzheimer's diseased tissue by synchrotron Fourier transform infrared microspectroscopy. *Biophys. J.* **71:** 1672–1679.

Chothia, C. 1973. Conformation of twisted β-pleated sheets in proteins. *J. Mol. Biol.* **75:** 295–302.

Chou, K.C. and Scheraga, H.A. 1982. Origin of the right-handed twist of β-sheets of poly(LVal) chains. *Proc. Natl. Acad. Sci.* **79:** 7047–7051.

Chou, K.C., Pottle, M., Nemethy, G., Ueda, Y., and Scheraga, H.A. 1982. Structure of β-sheets. Origin of the right-handed twist and of the increased stability of antiparallel over parallel sheets. *J. Mol. Biol.* **162:** 89–112.

Dong, A., Caughey, W.S., and Du Clos, T.W. 1994. Effects of calcium, magnesium, and phosphorylcholine on secondary structures of human C-reactive protein and serum amyloid P component observed by infrared spectroscopy. *J. Biol. Chem.* **269:** 6424–6430.

Dong, A., Matsuura, J., Allison, S.D., Chrisman, E., Manning, M.C., and Carpenter, J.F. 1996. Infrared and circular dichroism spectroscopic characterization of structural differences between β-lactoglobulin A and B. *Biochemistry* **35:** 1450–1457.

Dukor, R.K., Pancoska, P., Keiderling, T.A., Prestrelski, S.J., and Arakawa, T. 1992. Vibrational circular dichroism studies of epidermal growth factor and basic fibroblast growth factor. *Arch. Biochem. Biophys.* **298:** 678–681.

Eneqvist, T., Andersson, K., Olofsson, A., Lundgren, E., and Sauer-Eriksson, A.E. 2000. The β-slip: A novel concept in transthyretin amyloidosis. *Mol. Cell* **6:** 1207–1218.

Fandrich, M. and Dobson, C.M. 2002. The behaviour of polyamino acids reveals an inverse side chain effect in amyloid structure formation. *EMBO J.* **21:** 5682–5690.

Fandrich, M., Forge, V., Buder, K., Kittler, M., Dobson, C.M., and Diekmann, S. 2003. Myoglobin forms amyloid fibrils by association of unfolded polypeptide segments. *Proc. Natl. Acad. Sci.* **100:** 15463–15468.

Fink, A.L. 1998. Protein aggregation: Folding aggregates, inclusion bodies and amyloid. *Fold. Des.* **3:** R9–R23.

Fraser, P.E., Nguyen, J.T., Inouye, H., Surewicz, W.K., Selkoe, D.J., Podlisny, M.B., and Kirschner, D.A. 1992. Fibril formation by primate, rodent, and Dutch-hemorrhagic analogues of Alzheimer amyloid β-protein. *Biochemistry* **31:** 10716–10723.

From, N.B. and Bowler, B.E. 1998. Urea denaturation of staphylococcal nuclease monitored by Fourier transform infrared spectroscopy. *Biochemistry* **37:** 1623–1631.

Fukuda, H., Arai, M., and Kuwajima, K. 2000. Folding of green fluorescent protein and the cycle3 mutant. *Biochemistry* **39:** 12025–12032.

Jackson, M. and Mantsch, H.H. 1991. Protein secondary structure from FT-IR spectroscopy: Correlation with dihedral angles from three-dimensional Ramachandran plots. *Can. J. Chem.* **69:** 1639–1642.

Janek, K., Behlke, J., Zipper, J., Fabian, H., Georgalis, Y., Beyermann, M., Bienert, M., and Krause, E. 1999. Water-soluble β-sheet models which self-assemble into fibrillar structures. *Biochemistry* **38:** 8246–8252.

Jaroniec, C.P., MacPhee, C.E., Astrof, N.S., Dobson, C.M., and Griffin, R.G. 2002. Molecular conformation of a peptide fragment of transthyretin in an amyloid fibril. *Proc. Natl. Acad. Sci.* **99:** 16748–16753.

Jaroniec, C.P., MacPhee, C.E., Bajaj, V.S., McMahon, M.T., Dobson, C.M., and Griffin, R.G. 2004. High-resolution molecular structure of a peptide in an amyloid fibril determined by magic angle spinning NMR spectroscopy. *Proc. Natl. Acad. Sci.* **101:** 711–716.

Jimenez, J.L., Guijarro, J.I., Orlova, E., Zurdo, J., Dobson, C.M., Sunde, M., and Saibil, H.R. 1999. Cryo-electron microscopy structure of an SH3 amyloid fibril and model of the molecular packing. *EMBO J.* **18:** 815–821.

Jimenez, J.L., Nettleton, E.J., Bouchard, M., Robinson, C.V., Dobson, C.M., and Saibil, H.R. 2002. The protofilament structure of insulin amyloid fibrils. *Proc. Natl. Acad. Sci.* **99:** 9196–9201.

Kelly, J.W., Colon, W., Lai, Z., Lashuel, H.A., McCulloch, J., McCutchen, S.L., Miroy, G.J., and Peterson, S.A. 1997. Transthyretin quaternary and tertiary structural changes facilitate misassembly into amyloid. *Adv. Protein Chem.* **50:** 161–181.

Krimm, S., and Bandekar, J. 1986. Vibrational spectroscopy and conformation of peptides, polypeptides, and proteins. *Adv. Protein Chem.* **38:** 181–364.

Kubelka, J. and Keiderling, T.A. 2001. Differentiation of β-sheet-forming structures: Ab initio-based simulations of IR absorption and vibrational CD for model peptide and protein β-sheets. *J. Am. Chem. Soc.* **123:** 12048–12058.

Laurine, E., Gregoire, C., Fandrich, M., Engemann, S., Marchal, S., Thion, L., Mohr, M., Monsarrat, B., Michel, B., Dobson, C.M., et al. 2003. Lithostathine quadruple-helical filaments form proteinase K-resistant deposits in Creutzfeldt-Jakob disease. *J. Biol. Chem.* **278:** 51770–51778.

Lopez De La Paz, M., Goldie, K., Zurdo, J., Lacroix, E., Dobson, C.M., Hoenger, A., and Serrano, L. 2002. De novo designed peptide-based amyloid fibrils. *Proc. Natl. Acad. Sci.* **99:** 16052–16057.

McCammon, M.G., Scott, D.J., Keetch, C.A., Greene, L.H., Purkey, H.E., Petrassi, H.M., Kelly, J.W., and Robinson, C.V. 2002. Screening transthyretin amyloid fibril inhibitors: Characterization of novel multiprotein, multiligand complexes by mass spectrometry. *Structure* **10:** 851–863.

Muga, A., Cistola, D.P., and Mantsch, H.H. 1993. A comparative study of the conformational properties of *Escherichia coli*-derived rat intestinal and liver fatty acid binding proteins. *Biochim. Biophys. Acta* **1162:** 291–296.

Nguyen, J., Baldwin, M.A., Cohen, F.E., and Prusiner, S.B. 1995. Prion protein peptides induce α-helix to β-sheet conformational transitions. *Biochemistry* **34:** 4186–4192.

Nilsson, M.R. and Raleigh, D.P. 1999. Analysis of amylin cleavage products provides new insights into the amyloidogenic region of human amylin. *J. Mol. Biol.* **294:** 1375–1385.

Oberg, K., Chrunyk, B.A., Wetzel, R., and Fink, A.L. 1994. Nativelike secondary structure in interleukin-1 β inclusion bodies by attenuated total reflectance FTIR. *Biochemistry* **33:** 2628–2634.

Panick, G. and Winter, R. 2000. Pressure-induced unfolding/refolding of ribonuclease A: Static and kinetic Fourier transform infrared spectroscopy study. *Biochemistry* **39:** 1862–1869.

Perutz, M.F., Pope, B.J., Owen, D., Wanker, E.E., and Scherzinger, E. 2002. Aggregation of proteins with expanded glutamine and alanine repeats of the glutamine-rich and asparagine-rich domains of Sup35 and of the amyloid β-peptide of amyloid plaques. *Proc. Natl. Acad. Sci.* **99:** 5596–5600.

Petkova, A.T., Ishii, Y., Balbach, J.J., Antzutkin, O.N., Leapman, R.D., Delaglio, F., and Tycko, R. 2002. A structural model for Alzheimer's β-amyloid fibrils based on experimental constraints from solid state NMR. *Proc. Natl. Acad. Sci.* **99:** 16742–16747.

Prestrelski, S.J., Arakawa, T., Kenney, W.C., and Byler, D.M. 1991. The secondary structure of two recombinant human growth factors, platelet-derived growth factor and basic fibroblast growth factor, as determined by Fourier-transform infrared spectroscopy. *Arch. Biochem. Biophys.* **285:** 111–115.

Richardson, J.S. 1981. The anatomy and taxonomy of protein structure. *Adv. Protein Chem.* **34:** 167–339.

Salemme, F.R. 1983. Structural properties of protein β-sheets. *Prog. Biophys. Mol. Biol.* **42:** 95–133.

Sayle, R.A. and Milner-White, E.J. 1995. RASMOL: Biomolecular graphics for all. *Trends Biochem. Sci.* **20:** 374.

Sebastiao, M.P., Saraiva, M.J., and Damas, A.M. 1998. The crystal structure of amyloidogenic Leu55 → Pro transthyretin variant reveals a possible pathway for transthyretin polymerization into amyloid fibrils. *J. Biol. Chem.* **273:** 24715–24722.

Serag, A.A., Altenbach, C., Gingery, M., Hubbell, W.L., and Yeates, T.O. 2001. Identification of a subunit interface in transthyretin amyloid fibrils: Evidence for self-assembly from oligomeric building blocks. *Biochemistry* **40:** 9089–9096.

Serpell, L.C., Fraser, P.E., and Sunde, M. 1999. X-ray fiber diffraction of amyloid fibrils. *Methods Enzymol.* **309:** 526–536.

Shamovsky, I.L., Ross, G.M., and Riopelle, R.J. 2000. Theoretical studies on the origin of β-sheet twisting. *J. Phys. Chem. B* **104:** 11296–11307.

Surewicz, W.K., Szabo, A.G., and Mantsch, H.H. 1987. Conformational prop-

erties of azurin in solution as determined from resolution-enhanced Fourier-transform infrared spectra. *Eur. J. Biochem.* **167:** 519–523.

Surewicz, W.K., Leddy, J.J., and Mantsch, H.H. 1990. Structure, stability, and receptor interaction of cholera toxin as studied by Fourier-transform infrared spectroscopy. *Biochemistry* **29:** 8106–8111.

Susi, H. and Byler, D.M. 1987. Fourier transform infrared study of proteins with parallel β-chains. *Arch. Biochem. Biophys.* **258:** 465–469.

Susi, H., Timasheff, S.N., and Stevens, L. 1967. Infrared spectra and protein conformations in aqueous solutions. I. The amide I band in H2O and D2O solutions. *J. Biol. Chem.* **242:** 5460–5466.

Swamy, M.J., Heimburg, T., and Marsh, D. 1996. Fourier-transform infrared spectroscopic studies on avidin secondary structure and complexation with biotin and biotin-lipid assemblies. *Biophys. J.* **71:** 840–847.

Timasheff, S.N., Susi, H., and Stevens, L. 1967. Infrared spectra and protein conformations in aqueous solutions. II. Survey of globular proteins. *J. Biol. Chem.* **242:** 5467–5473.

Toniolo, C. and Palumbo, M. 1977. Solid-state infrared absorption spectra and chain arrangement in some synthetic homooligopeptides in the intermolecularly hydrogen-bonded pleated-sheet β-conformation. *Biopolymers* **16:** 219–224.

Villegas, V., Zurdo, J., Filimonov, V.V., Aviles, F.X., Dobson, C.M., and Serrano, L. 2000. Protein engineering as a strategy to avoid formation of amyloid fibrils. *Protein Sci.* **9:** 1700–1708.

Wilkins, D.K., Dobson, C.M., and Gross, M. 2000. Biophysical studies of the development of amyloid fibrils from a peptide fragment of cold shock protein B. *Eur. J. Biochem.* **267:** 2609–2616.

Yang, A.S. and Honig, B. 1995. Free energy determinants of secondary structure formation: II. Antiparallel β-sheets. *J. Mol. Biol.* **252:** 366–376.

Zscherp, C., Aygun, H., Engels, J.W., and Mantele, W. 2003. Effect of proline to alanine mutation on the thermal stability of the all-β-sheet protein tendamistat. *Biochim. Biophys. Acta* **1651:** 139–145.

Zurdo, J., Guijarro, J.I., and Dobson, C.M. 2001. Preparation and characterization of purified amyloid fibrils. *J. Am. Chem. Soc.* **123:** 8141–8142.